Supporting Information

Selective Enhancement of Methane Formation in Electrochemical CO_2 Reduction Enabled by a Raman-Inactive Oxygen-Containing Species on Cu

Ming He[1], Xiaoxia Chang[2,3,4], Tzu-Hsuan Chao[5], Chunsong Li[1], William A. Goddard III[6], Mu-jeng Cheng[5], Bingjun Xu[2,3,4] & Qi Lu[1]

[1]State Key Laboratory of Chemical Engineering, Department of Chemical Engineering, Tsinghua University, Beijing 100084, China

[2]College of Chemistry and Molecular Engineering, Peking University, Beijing 100871, China

[3]Beijing National Laboratory for Molecular Sciences, Beijing 100871, China

[4]Center for Catalytic Science and Technology, Department of Chemical and Biomolecular Engineering, University of Delaware, Newark, Delaware 19716, United States

[5]Department of Chemistry, National Cheng Kung University, Tainan 701, Taiwan

[6]Materials and Process Simulation Center, California Institute of Technology, Pasadena, California 91125, United States

*Corresponding author E-mails: mjcheng@mail.ncku.edu.tw; b_xu@pku.edu.cn; luqicheme@mail.tsinghua.edu.cn

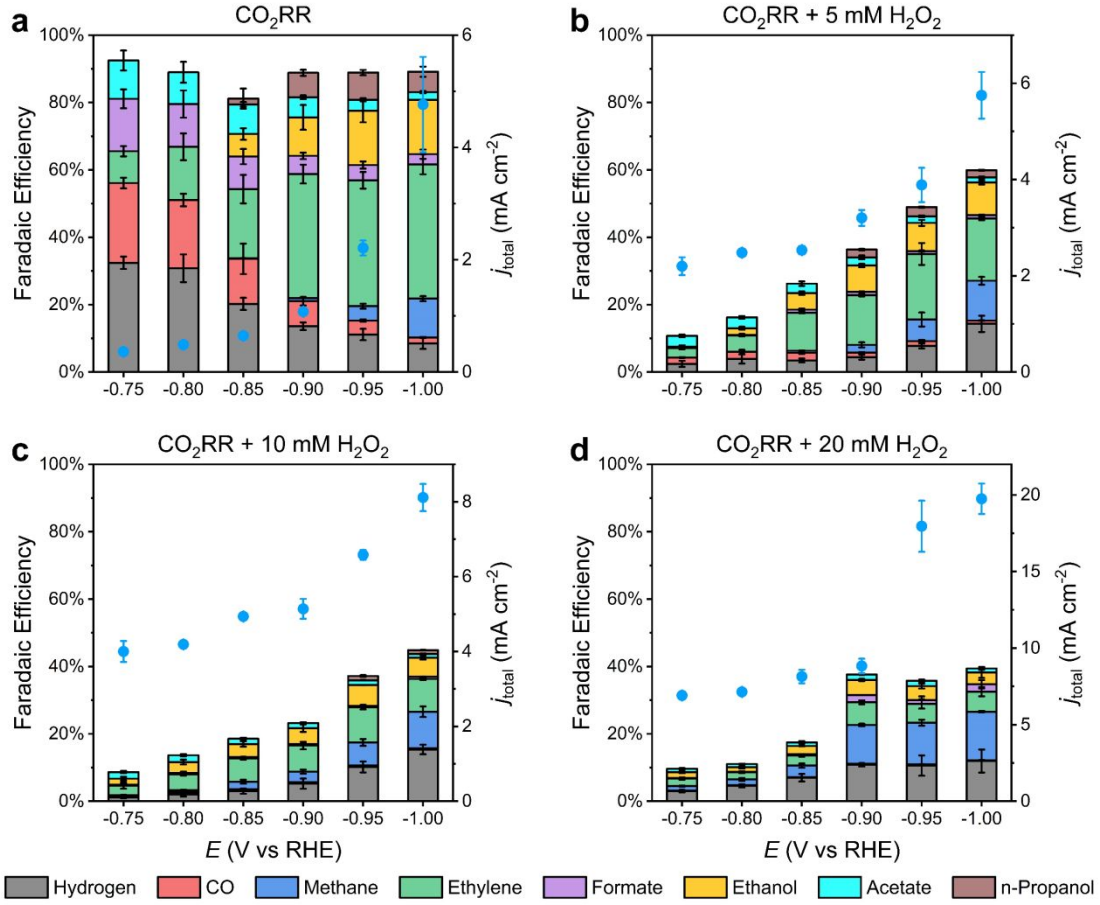

Figure S1. Total current densities and Faradaic efficiencies of the electropolished Cu foil electrode. The total current densities and Faradaic efficiencies are measured in (a) H_2O_2-free 0.1 M $KHCO_3$, (b) 0.1 M $KHCO_3$ with 5 mM H_2O_2, (c) 0.1 M $KHCO_3$ with 10 mM H_2O_2, (d) 0.1 M $KHCO_3$ with 20 mM H_2O_2. The error bars represent the standard deviation from at least three independent measurements. The missing parts of Faradaic efficiency in H_2O_2 induced experiments are attributed to H_2O_2 reduction.

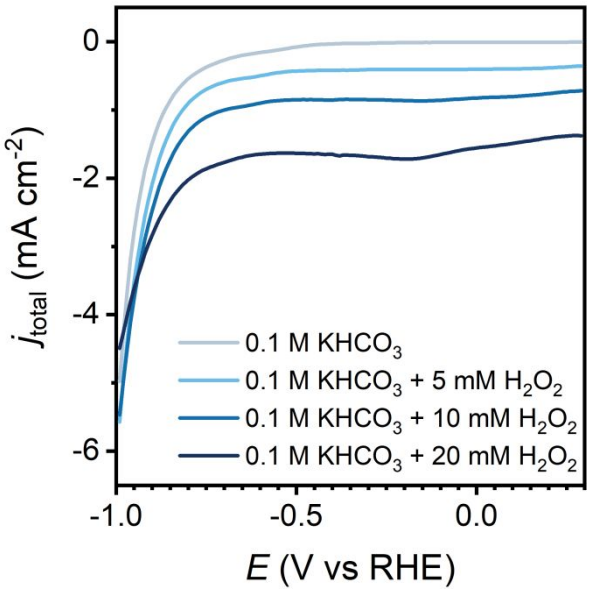

Figure S2. Linear sweep voltammograms from 0.3 V_{RHE} to -1 V_{RHE} in 0.1 M $KHCO_3$ + x mM H_2O_2 (x=0, 5, 10, 20). The experiments are conducted without stirring.

At > -0.65 V_{RHE}, the plateau-shape current densities are most likely due to the mass transport-limited reduction of H_2O_2, and differences can be attributed to the different H_2O_2 concentration. In 20 mM H_2O_2 added electrolyte, a broad reduction peak at ~ -0.2 V_{RHE} was observed. This could be attributed to the reduction of surface Cu oxide formed due to the addition of the largest amount of oxidative H_2O_2. At < -0.65 V_{RHE}, significant increase in current density can be observed due to the onset of HER and CO_2RR, which smears out the difference of mass transport-limited H_2O_2 reduction current.

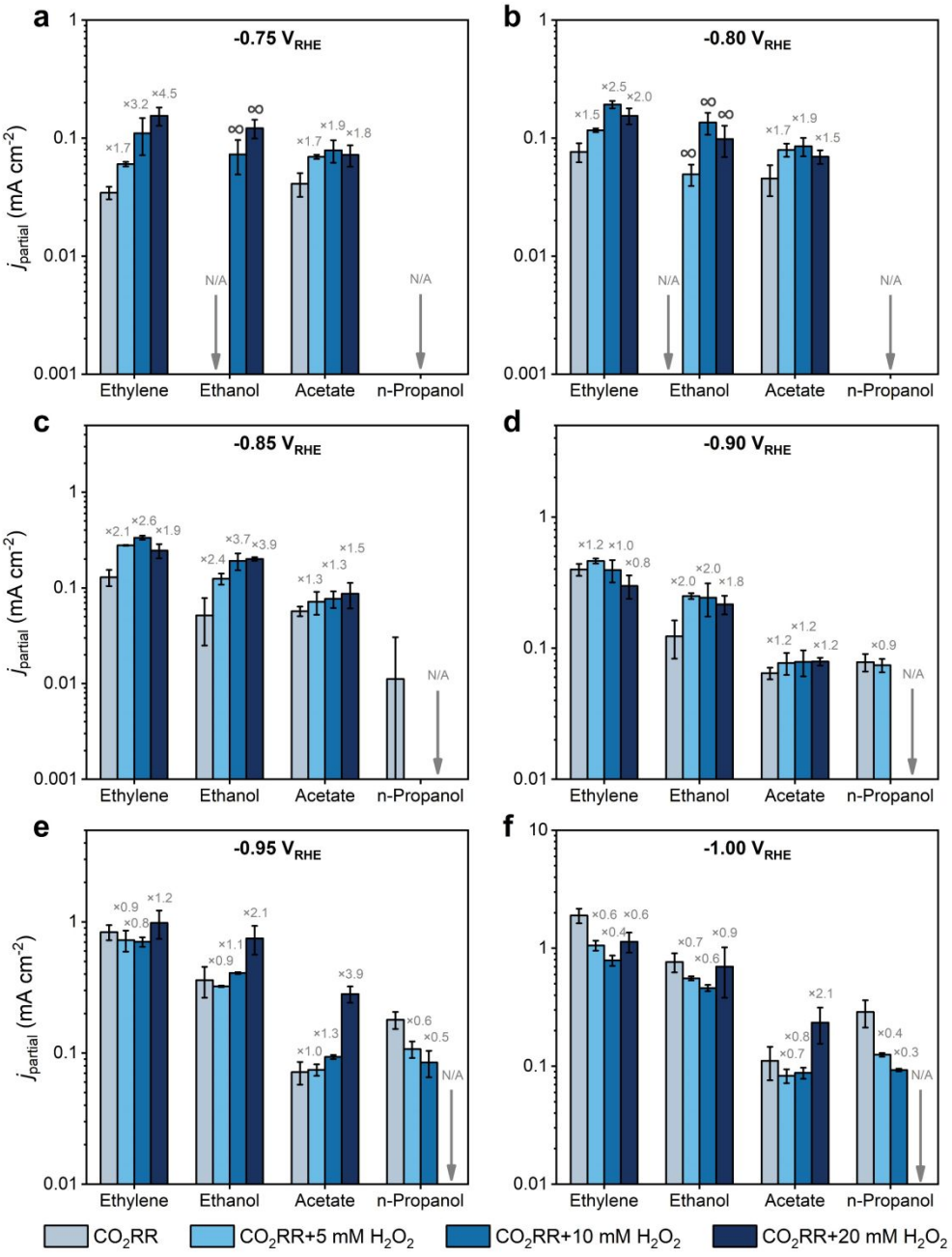

Figure S3. The partial current densities of ethylene, ethanol, acetate and n-propanol production. The partial current densities are measured in H_2O_2-free 0.1 M $KHCO_3$ and 0.1 M $KHCO_3$ with 5 mM, 10 mM, 20 mM H_2O_2. The partial current densities are compared at different potentials of (a) -0.75 V_{RHE}, (b) -0.80 V_{RHE}, (c) -0.85 V_{RHE}, (d) -0.90 V_{RHE}, (e) -0.95 V_{RHE}, (f) -1.00 V_{RHE}. The numbers stand for the enhancement relative to the rates in H_2O_2-free 0.1 M $KHCO_3$. 'N/A' represents that the product is not detected. The error bars represent the standard deviation from at least three independent measurements.

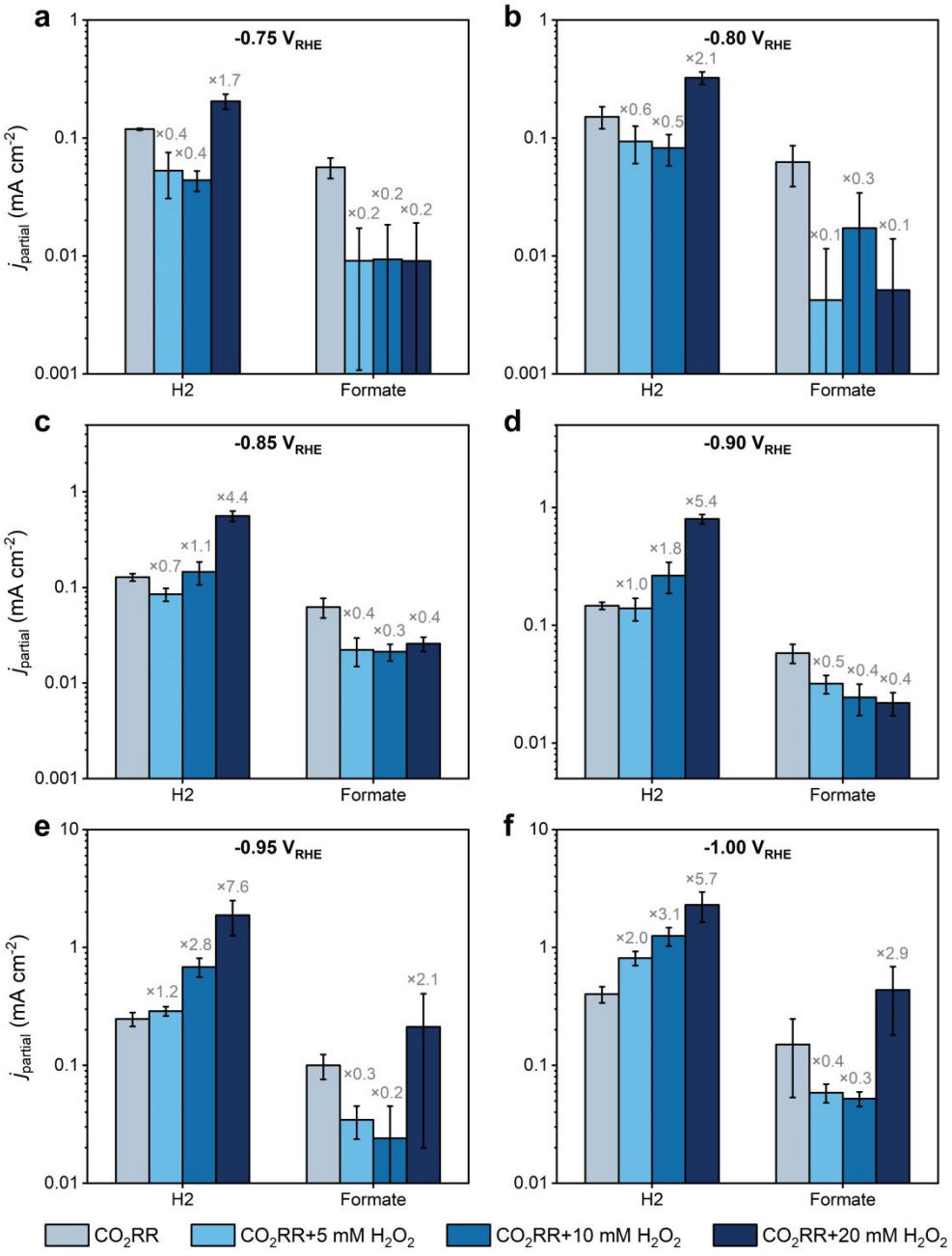

Figure S4. The partial current densities of hydrogen and formate production. The partial current densities are measured in H_2O_2-free 0.1 M $KHCO_3$ and 0.1 M $KHCO_3$ with 5 mM, 10 mM, 20 mM H_2O_2. The partial current densities are compared at different potentials of (a) -0.75 V_{RHE}, (b) -0.80 V_{RHE}, (c) -0.85 V_{RHE}, (d) -0.90 V_{RHE}, (e) -0.95 V_{RHE}, (f) -1.00 V_{RHE}. The numbers stand for the enhancement relative to the rates in H_2O_2-free 0.1 M $KHCO_3$. The error bars represent the standard deviation from at least three independent measurements.

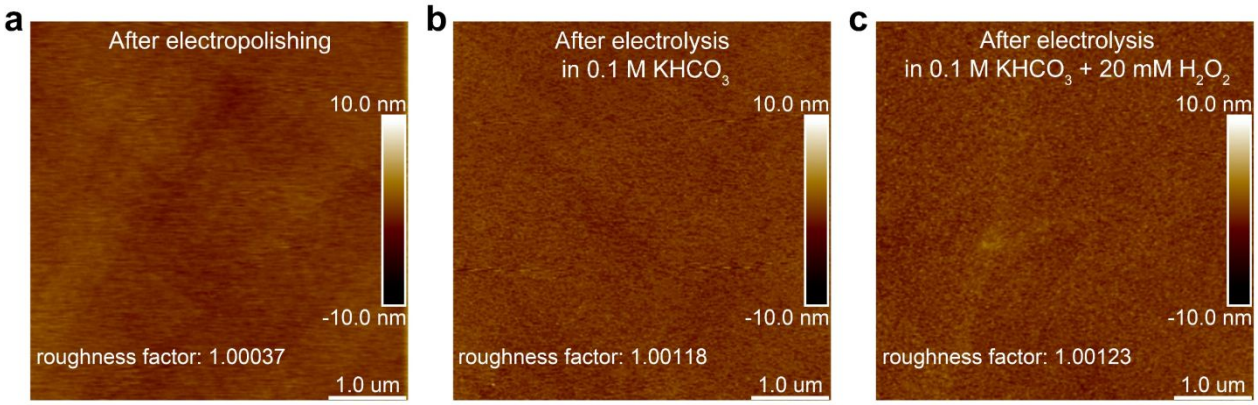

Figure S5. AFM images of (a) as-prepared Cu foil, (b) Cu foil after electrolysis in 0.1 M $KHCO_3$, and (c) Cu foil after electrolysis in 0.1 M $KHCO_3$ + 20 mM H_2O_2.

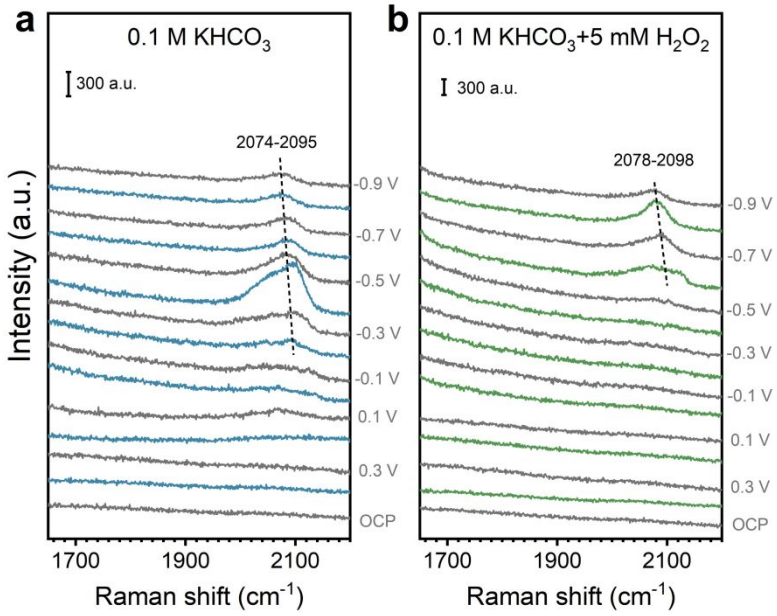

Figure S6. In situ shell-isolated nanoparticle-enhanced Raman spectra of C-O stretch region on electropolished Cu foil. The spectra are acquired at different potentials in CO_2 saturated (a) 0.1 M $KHCO_3$, (b) 5 mM H_2O_2 + 0.1 M $KHCO_3$, the electrolyte is continuously delivered into Raman cell during electrolysis. Peaks at 2074-2098 cm^{-1} can be assigned to the C-O stretching mode of atop CO.[1-2] No significant change in the frequency of C-O stretching mode can be observed in the absence or presence of H_2O_2. The potential at which the C-O stretching mode emerges becomes more negative after adding H_2O_2, which is due to the reduction of Cu_2O_{surf} requires more negative potential with the addition of H_2O_2. This is also consistent with the trend of Cu-C stretching (355 cm^{-1}) and rotation (296-303 cm^{-1}) mode of adsorbed CO (Figure 3).

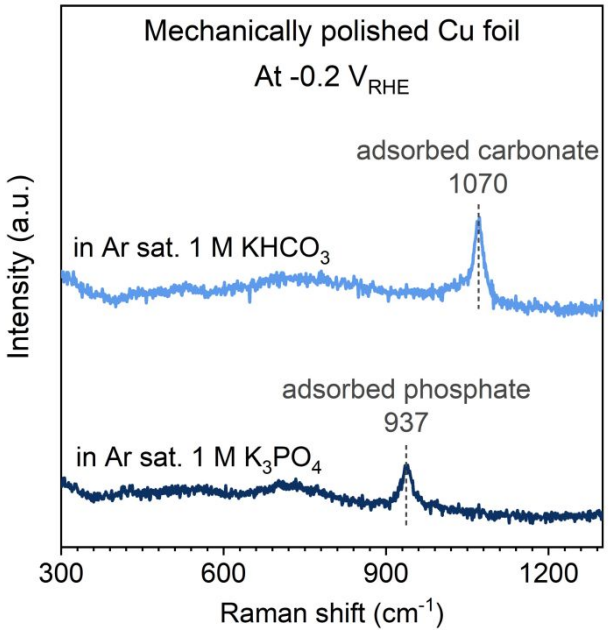

Figure S7. In situ surface-enhanced Raman spectra on mechanically polished Cu foil. The Cu foil is mechanically polished with 400 mesh sandpaper and rinsed thoroughly before electrolysis. The spectra are acquired at -0.2 V_{RHE} in Ar saturated 1 M $KHCO_3$ and 1 M K_3PO_4, respectively. The 937 cm^{-1} peak is absent in the $KCHO_3$ electrolyte, and the 1070 cm^{-1} peak is attributed to the adsorbed carbonate. SHINER particles are not employed in this experiment for the mechanically polished Cu foil readily exhibited surface enhancement. The electrolyte is continuously delivered into Raman cell during electrolysis.

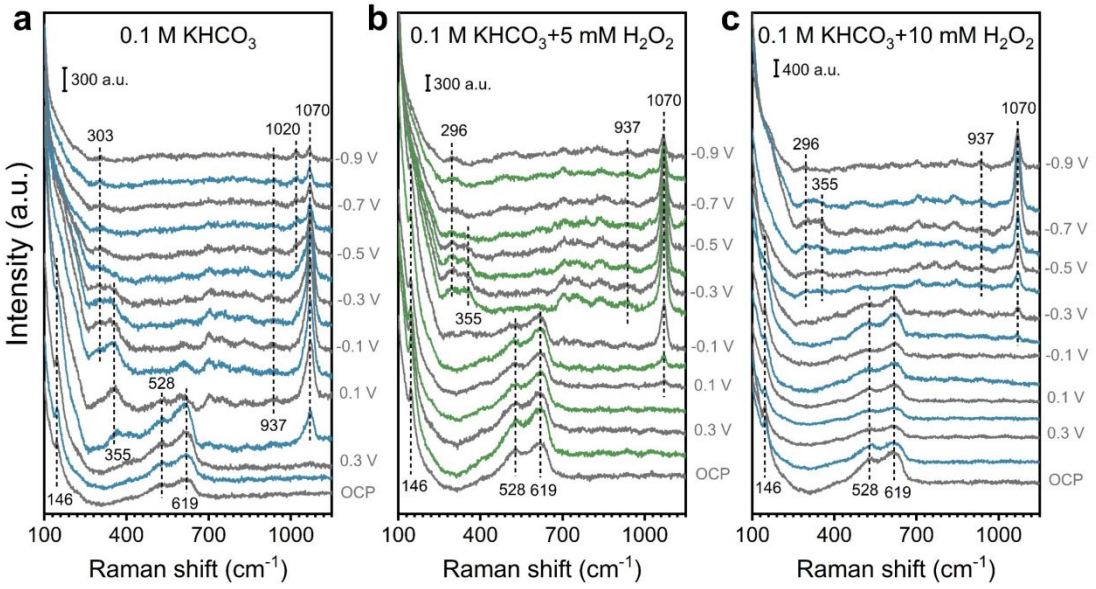

Figure S8. In situ shell-isolated nanoparticle-enhanced Raman spectra of electropolished Cu foil. The spectra are acquired at different potentials in CO_2 saturated (a) 0.1 M $KHCO_3$, (b) 5 mM H_2O_2 + 0.1 M $KHCO_3$, (c) 10 mM H_2O_2 + 0.1 M $KHCO_3$. The electrolyte is saturated with CO_2 before electrolysis and not continuously purged with CO_2 during electrolysis. The 1070 cm^{-1} peak appears at more negative potentials with the addition of H_2O_2, likely due to the carbonate adsorption is not favored on Cu_2O_{surf}, which can withstand more negative potentials in H_2O_2-containing electrolytes.

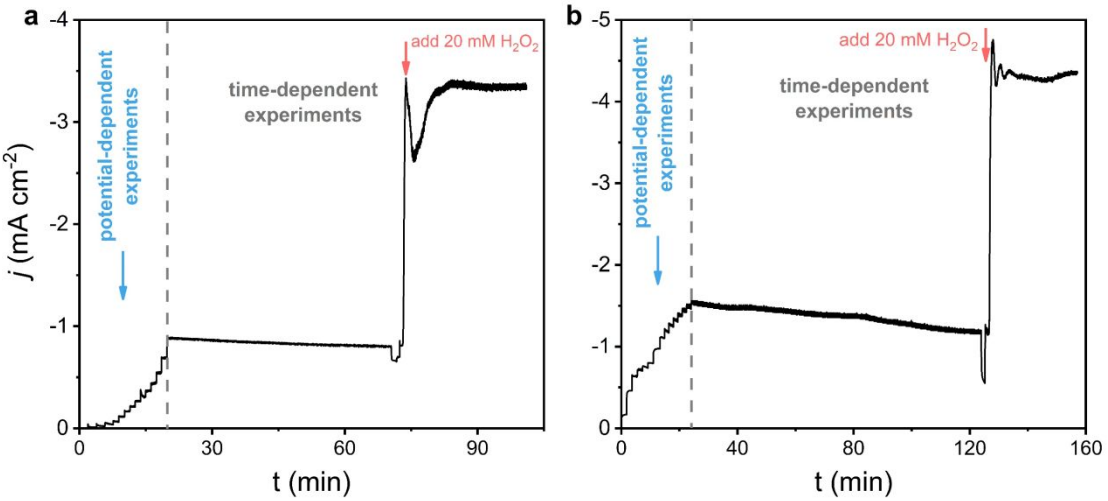

Figure S9. Current profiles of potential-dependent and time resolved in situ surface enhanced Raman studies. (a) 0.1 M $KHCO_3$, (b) 5 mM H_2O_2 + 0.1 M $KHCO_3$.

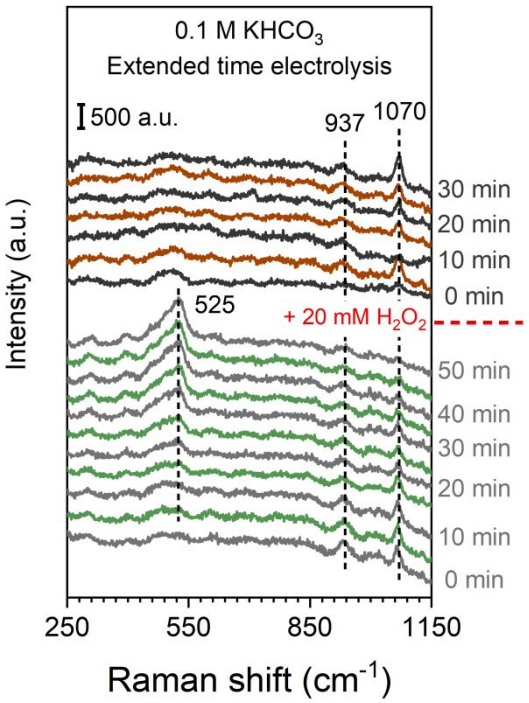

Figure S10. Time resolved in situ surface-enhanced Raman spectra of 250-1150 cm^{-1} at -1.0 V_{RHE} in 0.1 M $KHCO_3$, with 20 mM H_2O_2 added to the electrolyte at 55 min. The electrolyte is constantly purged with CO_2 during electrolysis.

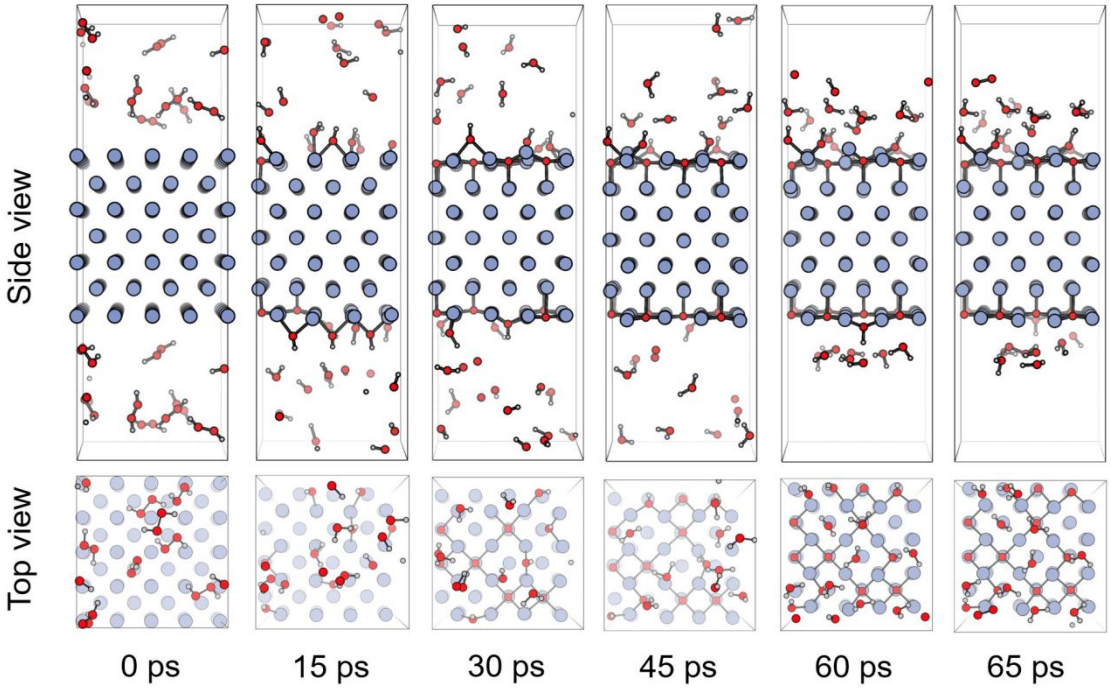

Figure S11. Structures of ReaxFF MD simulations for Cu(100) with H_2O_2. The blue, red, and white balls stand for copper, oxygen, and hydrogen atoms, respectively.

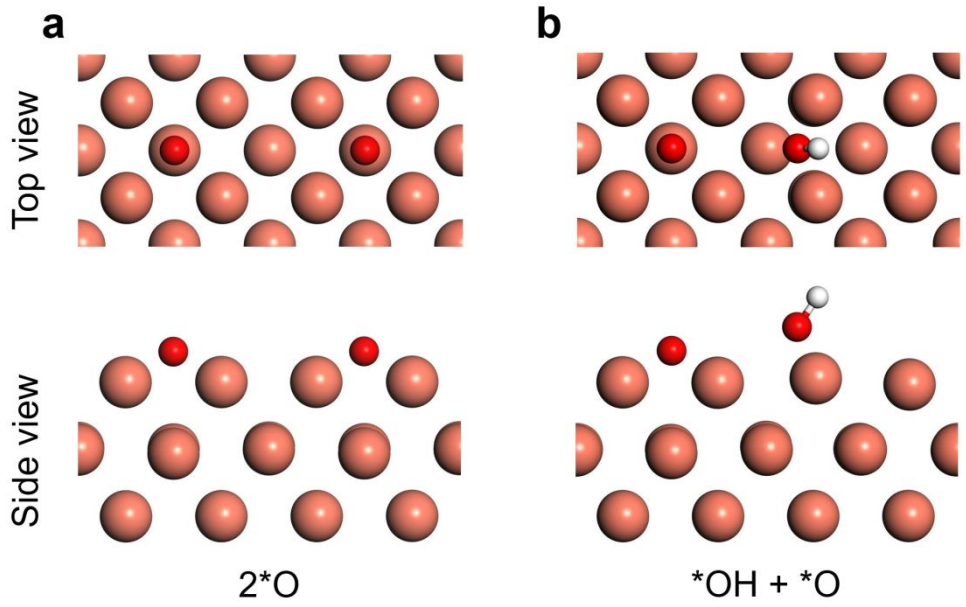

Figure S12. Structures of the models for Raman cross section calculations. (a) 2*O, (b) *OH + *O. The orange, red, and white balls stand for copper, oxygen, and hydrogen atoms, respectively.

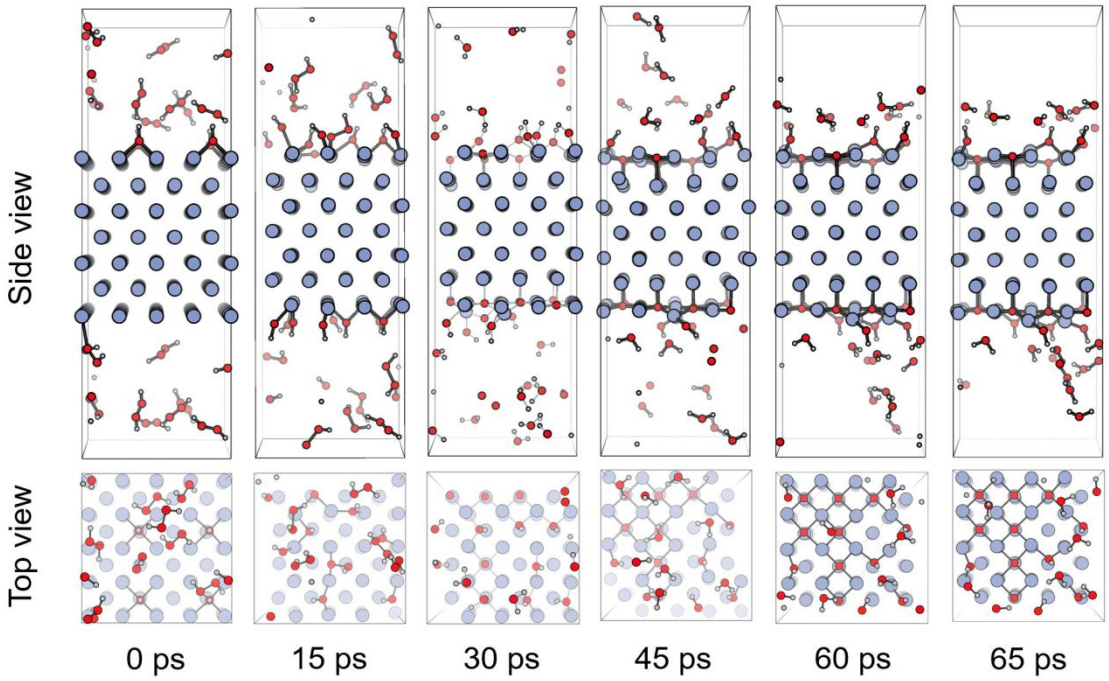

Figure S13. Structures of ReaxFF MD simulations for OH adsorbed Cu(100) with H_2O_2. The blue, red, and white balls stand for copper, oxygen, and hydrogen atoms, respectively.

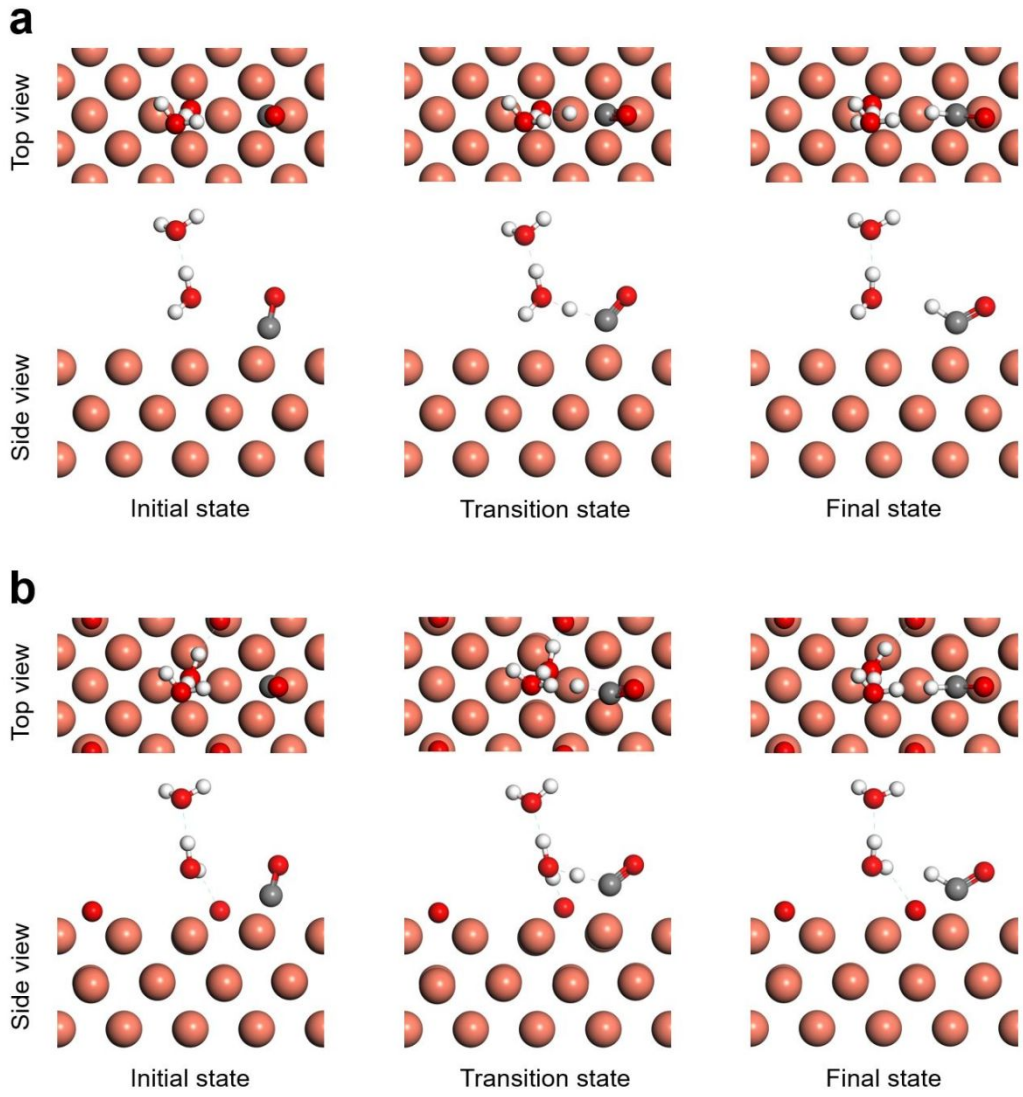

Figure S14. Structures of the initial state, transition state and final state of *CO hydrogenation on different surfaces. (a) Cu(100), (b) the 2*O surface. The orange, red, grey, and white balls stand for copper, oxygen, carbon and hydrogen atoms, respectively.

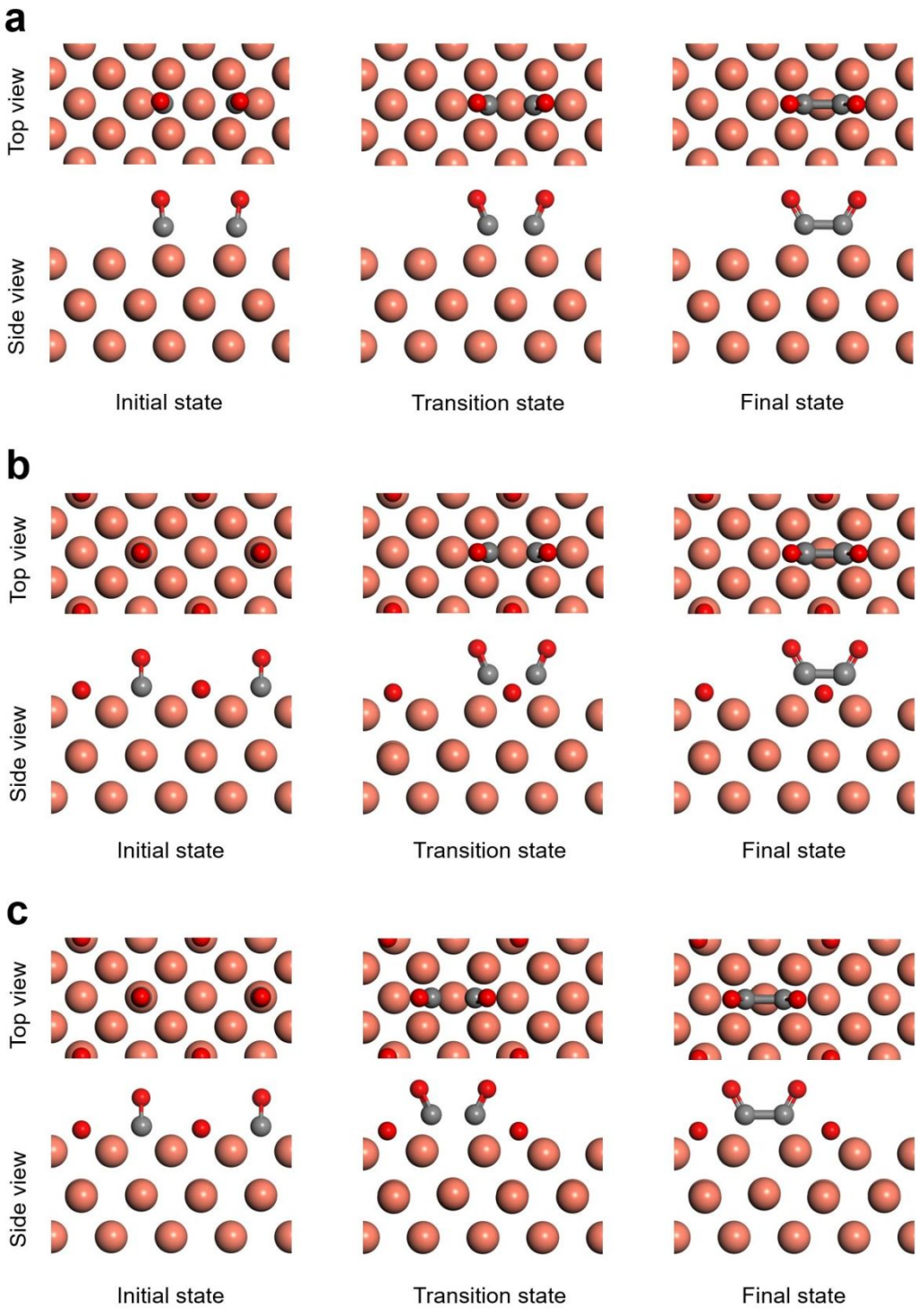

Figure S15. Structures of the initial state, transition state and final state of *CO dimerization on different surfaces. (a) Cu(100), (b) the 2*O surface (case 1), (c) the 2*O surface (case 2). The orange, red, and grey balls stand for copper, oxygen, and carbon atoms, respectively.

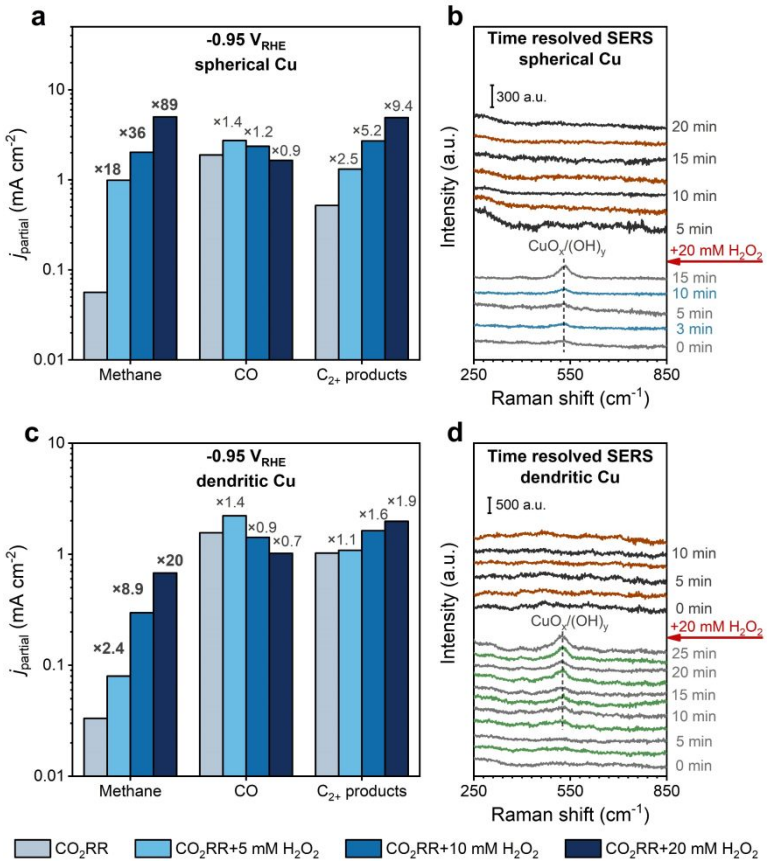

Figure S16. The partial current densities of CH_4, C_{2+} products and CO production and time resolved Raman spectra on spherical Cu and dendritic Cu. The partial current densities are measured at -0.95 V_{RHE} in H_2O_2-free 0.1 M $KHCO_3$ and 0.1 M $KHCO_3$ with 5 mM, 10 mM, 20 mM H_2O_2 on (a) spherical Cu and (c) dendritic Cu. Time resolved in situ surface-enhanced Raman spectra are acquired at -1 V_{RHE} in 0.1 M $KHCO_3$ on (b) spherical Cu and (d) dendritic Cu, with additional 20 mM H_2O_2 added to the electrolyte at 15 min and 25 min, respectively. The electrolyte is constantly purged with CO_2 during electrolysis.

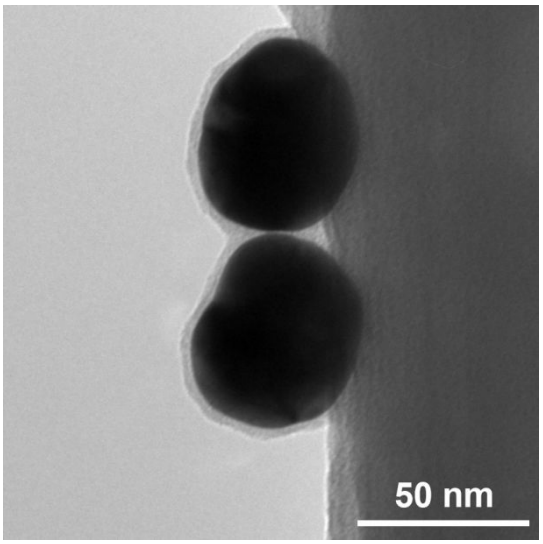

Figure S17. TEM image of the SHINER particles showing that the Au nanoparticles are completely covered by ~ 2 nm thick SiO_2 shell.

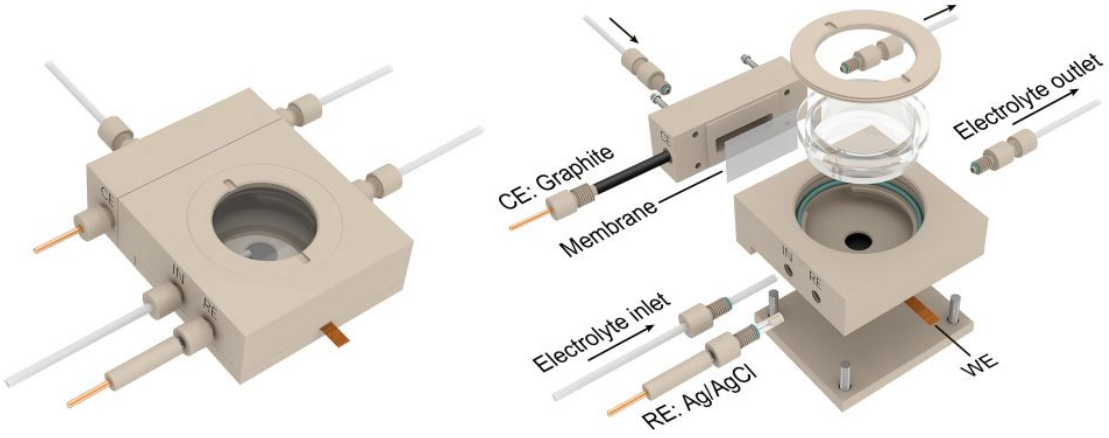

Figure S18. Schematic diagram of the SERS flow cell for in situ Raman spectroscopy measurements.

References

(1) Moradzaman, M.; Mul, G., In Situ Raman Study of Potential-Dependent Surface Adsorbed Carbonate, CO, OH, and C Species on Cu Electrodes During Electrochemical Reduction of CO_2. *ChemElectroChem* **2021,** *8* (8), 1478-1485.
(2) Chang, X. X.; Zhao, Y. R.; Xu, B. J., pH Dependence of Cu Surface Speciation in the Electrochemical CO Reduction Reaction. *ACS Catal.* **2020,** *10* (23), 13737-13747.